Phonons in polymorphous PbTe films. I. Infrared reflectivity of PbTe films on KCl substrates

1992 J. Phys.: Condens. Matter 4 4633

(http://iopscience.iop.org/0953-8984/4/19/006)

J. Phys.: Condens. Matter 4 (1992) 4633–4644. Printed in the UK

Phonons in polymorphous PbTe films: I. Infrared reflectivity of PbTe films on KCl substrates

M Baleva, L Bozukov and M Momtchilova
Faculty of Physics, University of Sofia, 1126 Sofia, Bulgaria

Received 28 August 1991

Abstract. PbTe films with various thicknesses, grown by laser-assisted deposition on KCl substrates, have been investigated. X-ray diffractograms have been taken in the angular range from 10° to 70°. FIR reflection spectra have been studied in the range from 20 to 5000 cm^{-1}. X-ray diffractograms indicated strained layers with HP PbTe phases: GeS and CsCl type. The frequencies of the infrared modes in these HP phases were determined by fitting the experimental spectra with the reflectance calculated for four media: air and two absorbing layers on absorbing substrate. It was found that the lineshape of the reflectance spectra was governed by a resonant-like frequency dependence of the electron damping parameter. The resonant-like shape of the damping parameter spectrum was attributed to electron scattering off potential wells, formed by dislocations.

1. Introduction

PbTe crystallizes with the NaCl-type (O_h^5) structure at ambient conditions. Pressure-induced structural phase transition from the NaCl-type phase to an intermediate orthorhombic phase (D_{2h}^{16} or D_{2h}^{17}) has been reported at a pressure between 4.5 and 6.0 GPa (Chattopadhyay *et al* (1986) and references therein). PbTe undergoes a further pressure-induced phase transition from the orthorhombic GeS-type phase to the CsCl-type (O_h^1) phase at 16 GPa (Fujii *et al* 1984). According to Wakabayashi *et al* (1968) the relative rates of change in the orthorhombic lattice parameters a, b and c for PbTe at the pressure of the phase transition (5 GPa) are 1.030, 0.931 and 0.926. The latter means that a change in the PbTe lattice constant of about 3% could lead to a phase transition. The mismatch between the PbTe ($a = 6.46$ Å) and KCl ($a = 6.29$ Å) lattice constants is about 3%. Then it can be expected that, when PbTe films are grown on KCl substrates, their crystal structure may be orthorhombic, at least in the initial stage of growth. PbTe films with GeS- and CsCl-type structures were grown by laser-assisted deposition (LAD) when the target material was doped with chromium (Baleva 1986). The crystal structure of those films was studied by electron diffraction (the electron penetration depth is about 40 Å). The fact that the orthorhombic GeS- or BCC CsCl-type phases were not detected in the undoped PbTe films does not strictly imply that the high-pressure (HP) phases did not exist in the films; it could also mean that the final stage of growth was always with a NaCl-type structure and did not depend on the film thickness. The presence of GeS- or CsCl-type phases in PbTe films, deposited on KCl substrates, can be detected by X-ray investigations. The phonon frequencies of the HP phases have to change significantly compared with the NaCl-type phases. The Raman-active phonon modes in GeS-type

0953-8984/92/194633 + 12 $04.50

phase of bulk PbTe have been studied by Ves *et al* (1989). It is impossible to investigate the infrared-active modes in bulk material under hydrostatic pressure. Thus the purpose of the work was both to detect the presence of HP PbTe phases by x-ray and far-infrared (FIR) reflectance investigations and to obtain the frequencies of the infrared-active modes in these HP phases.

2. Samples and experimental results

2.1. Samples

PbTe films were grown by LAD on KCl(100) substrates. The technological conditions, which can be varied in the LAD, are substrate temperature T_s, laser energy per pulse E_p and substrate-to-target distance L. The carrier concentration was calculated from the Hall coefficient and the electrical conductivity measured by Van der Pauw's method. The film thicknesses were determined from the pictures of the cross-sections, taken with an electron scanning microscope (magnification, 25 000). The data on three of the samples, which were investigated in detail, are given in table 1.

A periodic modulation of the interference transmittance and reflectance spectra of the PbTe/KCl fims was usually observed. The periodic modulation can be caused by an additional layer with optical constants and thickness which differ from those of the basic film. In figure 1 the modulated transmittance spectrum of sample 1010 is shown. The thickness of the additional (*strained*) layer, which can be easily evaluated from the spectrum (on the assumption of the same refractive indices for both layers), is about 0.5 μm, while the thickness of the basic (*relaxed*) film is 2.1 μm. In order to investigate the crystal structure of the strained layer, x-ray measurements were undertaken.

2.2. X-ray diffraction

The x-ray diffraction patterns were taken using a standard x-ray diffractometer URD-6 with Cu Kα radiation, with a graphite monochromator and with a step size of 0.02°. The angular range varied from 10° to 70°. The lattice constants and the calculated values of peak intensities were obtained using the PULVERIX program as implemented by H Möller, Institut für Experimentalphysik, Technische Universität, 1040 Wien, Austria. Figure 2 shows the diffraction patterns of the films with various thicknesses. These diffractograms indicate mainly a NaCl-type structure with a (100) direction of crystallization. The latter means that the upper sublayer in all the films crystallizes in the NaCl-type structure. The lattice constant for the NaCl-type unit cell is $a = 6.455 \pm 0.003$ Å in very good agreement with that determined by Chattopadhyay *et al* (1986) ($a = 6.458$ Å) at a pressure $P =$ 0.5 GPa. The (200) and (400) reflections of the KCl substrate with intensities increasing on decrease in the film thickness are clearly resolved as well. The KCl peaks obviously follow strictly the Kα doublet of the Cu as they are split. It is known that this indicates a perfect single-crystal structure and a good resolution of the set-up. In figure 3 the same diffraction patterns are shown at a magnification of about 10^3 times. In the figure, additional reflections, which cannot be indexed in the NaCl-type structure, are clearly resolved. The intensities of the additional reflections are about three orders of magnitude lower than the NaCl(200)- and NaCl(400)-type structure reflections. Thus it is reasonable to attribute these reflections to the expected strained sublayers, formed in the initial stage of growth. We succeeded in indexing these reflections for the HP PbTe phases: GeS- and CsCl-type structures. The lattice parameters of the orthorhombic phase a, b

Table 1. Samples, growth conditions and lattice parameters of the high-pressure PbTe phases.

Sample	Thickness		Technological conditions			Carrier concentration	Lattice constant				
							GeS-type phase			CsCl-type phase	
	d (μm)	d_{FCC}/d_{HP}	T_s (°C)	E_p (J)	L (cm)	p (10^{17} cm^{-3})	a (Å)	b (Å)	c (Å)	a (Å)	$I_{CsCl(100)}/I_{GeS(200)}$
1010	2.6	2.1/0.5	250	2.5	2	0.6	—	—	—	3.581	0.3
0910	0.9	0.6/0.3	250	2.4	2	4.2	4.699	11.460	4.357	3.576	7.0
1411	0.1	0.05/0.05	200	4.8	3	5.7	4.697	11.620	4.345	3.567	0.2

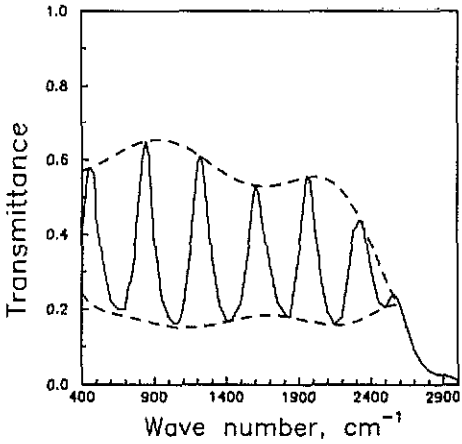

Figure 1. The transmittance spectrum of the sample 1010.

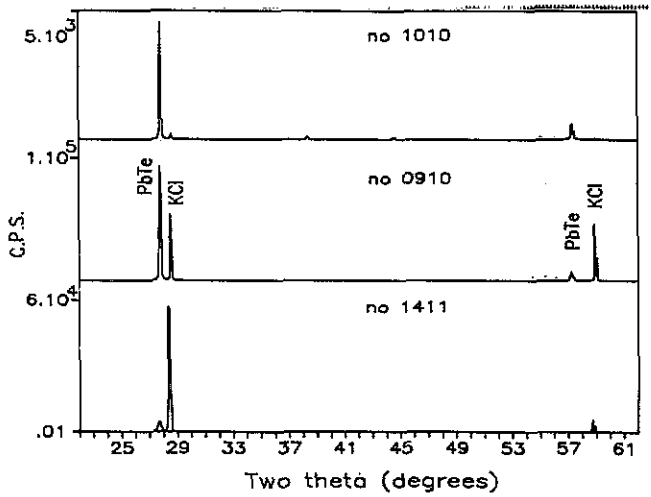

Figure 2. X-ray diffraction spectra of PbTe films with various thicknesses. The intensities are given in counts per second (C.P.S.).

and c as well as the parameter of the BCC CsCl-type phase for the various samples are given in table 1. In figure 4 the experimental x-ray spectrum of sample 0910 (figure 4(a)) is compared with the calculated lines in the spectra. The vertical bars in figure 4(b) represent the intensities of the reflections in the NaCl-type phase in the (100) directions; the intensities of the reflections in a polycrystal GeS-type phase calculated by the use of the same atomic positions of Pb and Te atoms as those in SnSe (as was done by Fujii *et al* (1984)) and with the parameters a, b and c for sample 0910 (see table 1) are shown in figure 4(d). Figure 4(c) represents the intensities of the reflections of CsCl-type phase crystallized in the (100) direction, calculated also with the parameter a for sample 0910. Thus the x-ray investigations indicated that the strained sublayers in PbTe films, deposited on KCl substrates, crystallized with the polycrystal GeS-type and single-crystal CsCl(100)-type structures. The fact that the GeS-type component is polycrystalline can be easily understood if one takes into account the equal probabilities of orientation of the GeS-phase c axis along one of the two possible directions of the cubic substrate surface.

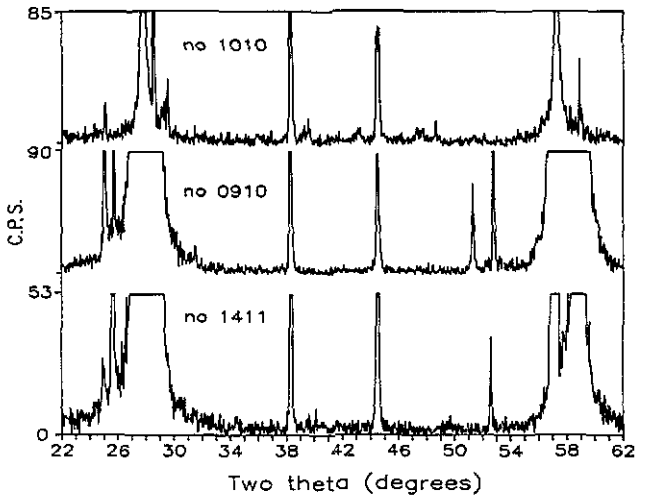

Figure 3. The same x-ray diffraction spectra as in figure 2, with a magnification of about 10^3 times.

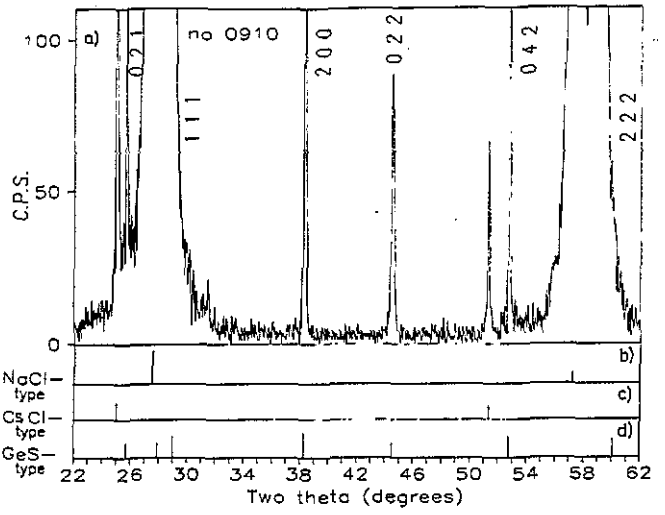

Figure 4. X-ray diffraction spectrum of sample 0910. The reflection intensities calculated for the (*b*) NaCl-, (*c*) CsCl- and (*d*) GeS-type PbTe phases are represented by vertical bars.

The reflection intensities of the HP phases (the content of the strained layer) in the various films are hidden to a different extent by the upper NaCl-type phase. Therefore the change in the thickness of the strained layer from one film to another cannot be followed. However, it is possible to evaluate the relative contents of CsCl- and GeS-type phase structures in the strained sublayer of the films. The relations between the intensities of the (100) reflection in the CsCl-type phase and the (200) reflection in the GeS-type phase are given in table 1. As is seen, the GeS-type phase prevails in samples 1010 and 1411 while the CsCl-type phase is dominant in sample 0910. The lattice parameters of the HP unit cells, with exception for the parameter *b* in the orthorhombic phase, are nearly the same in all samples. Thus the growth technological conditions,

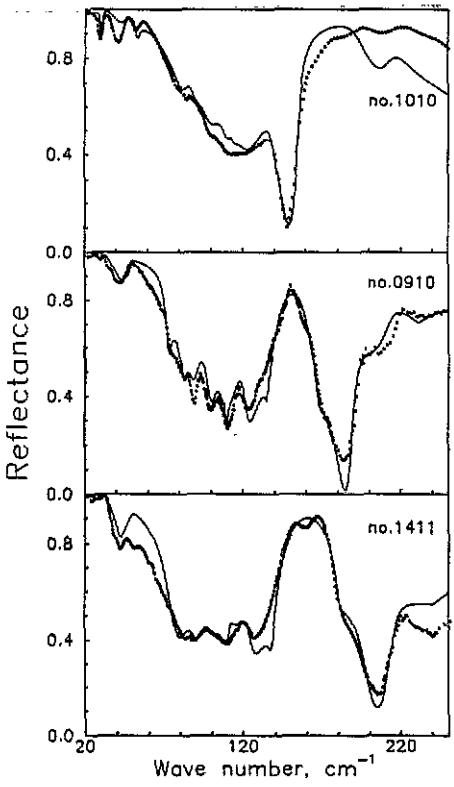

Figure 5. The experimental (· · ·) and calculated (——) reflectance spectra of three samples with various thicknesses.

which are different for the various samples, influence the HP phase quantity more strongly than the lattice parameters.

2.3. *Far-infrared reflectance*

FIR reflectance spectra for light at nearly normal incidence were taken using a Bomem Fourier spectrometer in the range from 20 to 5000 cm^{-1} at room temperature.

In figure 5 the reflectance spectra of the investigated films are shown in the range from 20 to 250 cm^{-1} (dotted curves). The experimental spectra were investigated by a fitting procedure. To calculate the reflectance spectra the following points have to be taken into account.

(i) *The film has to be considered as a two-layer structure*: a relaxed sublayer with a NaCl-type structure, and a strained sublayer consisting of GeS- and CsCl-type phases. Then multiple reflections from two absorbing films on an absorbing substrate have to be calculated. The reflectivity from four media (including air) for light of normal incidence is given by the relation (Kondrashov 1976)

$$R_{14} = [R_{12} + 2\sqrt{R_{12}R_{24}}\exp(-\alpha_2 d_2)\cos(2\delta_2 + \varphi_{12} - \varphi_{24}) + R_{24}\exp(-2\alpha_2 d_2)] \times [1 + 2\sqrt{R_{12}R_{24}}\exp(-\alpha_2 d_2)\cos(2\delta_2 - \varphi_{12} - \varphi_{24}) + R_{12}R_{24}\exp(-2\alpha_2 d_2)]^{-1} \tag{1}$$

where

$$R_{m(m+1)} = r_{m(m+1)}r^*_{m(m+1)} = [(n_m - n_{m+1})^2 + (\kappa_m - \kappa_{m+1})^2]/[(n_m + n_{m+1})^2 + (\kappa_m + \kappa_{m+1})^2]$$

Table 2. The parameters for the phonon modes obtained by the fitting procedure.

	Sample 1010		Sample 0910		Sample 1411		
	$\omega_{t,j}$ (cm^{-1})	γ_j	$\omega_{t,j}$ (cm^{-1})	γ_j	$\omega_{t,j}$ (cm^{-1})	γ_j	s_j
FCC PbTe	32	1	32	1	32	1	350
BCC PbTe	50	2	50	3	50	10	106
Orthorhombic	46	2	46	3	46	10	7
	84	8	84	8	84	12	1.8
	92	14	92	8	95	12	1.8
PbTe	104	14	104	8	105	12	0.9
	118	14	118	10	122	12	0.6
	134	14	134	10	136	12	0.6

$\delta_m = (2\pi/\lambda)n_m d_m \qquad \alpha_m = (4\pi/\lambda)\kappa_m.$

The change in the phase at the boundary between two media m and $m+1$ is

$$\varphi_{m(m+1)} = \tan^{-1}[\mathrm{Im}(r_{m(m+1)})/\mathrm{Re}(r_{m(m+1)})]$$
$$= \tan^{-1}\{2(n_m\kappa_{m+1} - n_{m+1}\kappa_m)/[(n_m^2 + \kappa_m^2) - (n_{m+1}^2 + \kappa_{m+1}^2)]\}$$

$m = (1, 2, 3)$.

The indices m in the above formulae are related to the media under consideration as follows: 1, air; 2, the relaxed PbTe sublayer; 3, the strained PbTe sublayer; 4, the KCl substrate. d_m is the thickness of the corresponding media and λ is the wavelength of the incident light. The reflectivity R_{24} was calculated from equation (1) where the indices 1 and 2 were replaced by 2 and 3, respectively.

The optical constants n_m and κ_m were calculated from the real and imaginary parts of the dielectric functions $\varepsilon_m(\omega)$. In the framework of the oscillator model with the Drude term the dielectric function of each of the absorbing media under consideration can be written in the form

$$\varepsilon(\omega) = \varepsilon_\infty + \sum_j \frac{s_j\omega_{t,j}^2}{\omega_{t,j}^2 - \omega^2 - i\gamma_{t,j}\omega} - \frac{\varepsilon_\infty\omega_p^2}{\omega(\omega + i\gamma_p)} \tag{2}$$

where ε_∞ is the optical dielectric constant, $\omega_{t,j}$ is the TO phonon frequency of the j oscillator, s is the j-oscillator strength, $\gamma_{t,j}$ is the oscillator damping, ω_p is the plasma frequency and γ_p is the free-carrier damping parameter.

The parameters for the KCl substrate were $\varepsilon_\infty = 2.18$, $\omega_t = 142\ cm^{-1}$, $s = 2.52$ and $\gamma_t = 7\ cm^{-1}$. These values, which are in excellent agreement with the results of other workers (Bruesch (1986) and references therein) were determined by fitting the experimental reflectance spectra of the substrate solely according to equations (1) and (2) written for two media (air and substrate).

The values of the oscillator frequencies and the oscillator strengths for which the best fit of the experimental spectra was obtained are given in table 2; the corresponding damping parameters are given in table 3.

As the upper film sublayer is of the NaCl type, only one TO phonon mode can be expected in it. The value of $32\ cm^{-1}$ obtained for all investigated samples is in good agreement with the experimental values for the phonon mode in PbTe, obtained by other workers for both film and bulk materials (Burkhard *et al* 1976, Perkowitz 1975).

The second film sublayer contains CsCl- and GeS-type phases. The CsCl-type crystal structure implies one TO mode. The mode at 50 cm^{-1} was attributed to the CsCl-type structure as the oscillator strength of this mode is much higher than the oscillator strengths of the remaining modes. A factor-group analysis predicts seven IR-active modes for the GeS-type structure. Therefore the remaining phonon modes detected were attributed to the strained sublayer. It should be noted that the half-width and oscillator strength cannot be determined unambiguously from the multioscillator fit in general. This is especially valid for our strained layer consisting of two phases. Therefore the phonon damping parameters and oscillator strengths given in table 2 can be regarded as effective values of these parameters.

(ii) It has been shown by a number of workers that the reflectivity lineshape in the investigated range is governed by *the frequency-dependent electron damping parameter* γ_p. The spectral dependence of the electron damping parameter in PbTe films on NaCl substrates in particular has been discussed by Burkhard *et al* (1978) and by Katayama *et al* (1983). Burkhard *et al* (1978) succeeded in interpreting the dip in their reflectance spectra near 150 cm^{-1} considering a strong resonant-like increase of the electron damping parameter in the region. This behaviour of the damping parameter according to Burkhard *et al* (1978) can be related to a power dissipation process caused by a plasmon–phonon–impurities interaction. Katayama *et al* (1983) found that in this material the contribution from the screened impurity–electron scattering is smaller than the scattering off the coupled plasmon–LO-phonon modes by two orders of magnitude.

The spectral dependence of the damping parameter has a resonant-like behaviour in the case of resonant electron scattering off potential wells. According to Ridley's (1986) theory the damping parameter frequency dependence in this case can be written in the form

$$\gamma_p(\omega) = b\Gamma^2[(\omega - \omega_r)^2 + \Gamma^2]^{-1} \tag{3}$$

where b depends on the potential well density and on the free-carrier effective mass, $\Gamma = (\omega_0\omega)^{1/2}$ is a frequency-dependent width of the resonant line, $\omega_0 \sim V_0 r_t$ (V_0 is the well potential and r_t is a characteristic size of the potential well) and $E_r = \hbar\omega_r$ is the energy of a bound state in the potential well. Potential wells in samples can be formed by dislocations in particular. The perturbation of the crystal field in the vicinity of the dislocation forms localized states under the conductivity band bottom or above the valence band top, depending on the conductivity type of the material. The interaction of these states with carriers in the surrounding area leads to the appearance of a depletion layer. The band bending as a result of dislocations has been proved experimentally by a number of workers. In the case of p-type Ge, absorption at energy $E_r = 0.1$ eV has been detected (Barth *et al* 1976). This absorption has been attributed to transitions from the valence band top to the localized dislocation state above it.

The probability of finding an electron in the energy gap away from the band edge decreases according to $\exp(-\omega/\omega_0)$. Then it is reasonable to assume that the linewidth Γ in equation (3) can be written in the form

$$\Gamma = (\omega_0\omega)^{1/2} \exp(-\omega/\omega_0). \tag{4}$$

The γ_p spectral dependences, calculated according to equation (3) with $\Gamma = (\omega_0\omega)^{1/2} \exp(-\omega/\omega_0)$ and $E_r = 0.0174$, 0.0166 and 0.0149 eV for the various samples, were used to obtain the best fit to the experimental spectra (figure 6). The values of the bound-state energy in PbTe is in an order of magnitude lower than that in Ge, which is quite natural if one takes into account that the static dielectric constant in

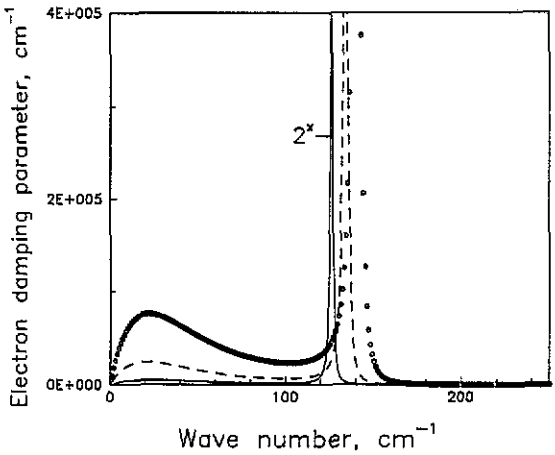

Figure 6. The frequency dependence of the electron damping parameter, calculated according to equations (3) and (4): O, sample 1411; - - -, sample 0910; ——, sample 1010.

Table 3. The parameters for electron damping.

Electron damping parameters	Value for the following samples		
	1010	0910	1411
b (10^5)	2	50	40
ω_r (cm^{-1})	128	138	150
ω_0 (cm^{-1})	28	28	32
ω_p (cm^{-1})	94	148	165

Ge is an order of magnitude lower than that in PbTe (16.3 as against 380). The value of the energy E_r depends on the Fermi level energy in the sample and as can be expected becomes smaller, the higher is the carrier concentration (see table 1). It is worth noting that the resonant energy of the electron damping frequency dependence assumed by Burkhard *et al* (1978) is of the same order: 0.021 eV.

The values of the parameters b, ω_r and ω_0, for which the best fit to the experimental spectra was obtained, are shown in table 3. The parameter b which depends on the dislocation density is higher for thinner samples, where the strained-layer thickness is comparable with that of the relaxed layer. In table 3 the values of the plasma frequencies ω_p of the various samples are included as well.

3. Discussion

3.1. Electron damping parameter

We succeeded in interpreting our experimental data, assuming like Burkhard *et al* (1978) a resonant-like increase in the damping parameter. However, from our point of view, the prevailing scattering mechanism in highly mismatched films is scattering off dislocations. We believe that the same scattering mechanism prevails in the PbTe/NaCl and PbTe/

BaF_2 films, investigated by Burkhard *et al* (1976, 1977, 1978). The mismatches between the lattice constants of PbTe and NaCl and between those of PbTe and BaF_2 are 14.3% and 4.3%, respectively, higher than between PbTe and KCl lattice constants. Contrary to LAD, the hot-wall growth technique is an equilibrium process. Nevertheless the thickness of the strained sublayers in the films investigated by Burkhard *et al* (1977) is comparable with that of our samples as a result of the higher mismatch between the PbTe and substrates that they used. A periodic modulation of the transmittance spectrum of sample PbTe/BaF_2 2385, shown in figure 1 in the paper by Burkhard *et al* (1976), can be easily seen. The thickness of the strained sublayer, which can be evaluated from the spectrum, is about 450 nm—comparable with the thickness of the strained layers in our films. What is more, this strained sublayer obviously contains a HP phase, as an additional phonon mode at 48 cm^{-1} has been reported. As is seen from table 2, we have detected phonon modes at 46 and 50 cm^{-1}.

Our assumption about the nature of the electron scattering mechanism is supported by the following experimental facts.

(i) The value of the damping parameter increases with decrease in the sample thickness (see figure 6).

(ii) The value of the damping parameter increases with decrease in the temperature, according to Burkhard *et al* (1978). This can be easily understood bearing in mind that mismatch between the lattice constants of PbTe and BaF_2 increases with temperature decrease, which thus increases the dislocation density.

(iii) Our investigations on the initial stage of the film growth by high-resolution electron microscope (Carl Zeiss Jena) indicate a high dislocation density (the data will be published elsewhere).

3.2. Assignment of the phonon modes

Taking into account the presence of the HP PbTe phases in all the samples a tentative assignment of the phonon modes, attributed to the strained sublayer, can be performed if one adopts the GeS-type structure for the orthorhombic PbTe and CsCl-type structure for the BCC PbTe. The zero-pressure phonon frequencies in orthorhombic IV–VI compounds such as GeS, GeSe, SnS and SnSe were approximately scaled by the expression (Ves *et al* 1989)

$$\omega_0 \sim V_0^{-N} M^{-1/2} \tag{5}$$

where V_0 is the specific volume at $P = 0$ GPa. M is the sum of the constituent atoms when calculating the low-frequency modes and the reduced mass for the high-frequency modes (Chandrasekhar *et al* 1977) and $N = 0.75$ in agreement with the value obtained from the experiment by Ves *et al* (1989). The phonon modes in orthorhombic PbTe were scaled from the SnSe mode frequencies as SnSe is one of the GeS-type compounds in which all the infrared modes have been detected and also as the atom positions in the orthorhombic PbTe when interpreting the x-ray diffractograms were taken to be the same as in SnSe. The specific SnSe volume was calculated from its lattice parameters at zero pressure (Chandrasekhar *et al* 1977). The specific volume of the orthorhombic PbTe ($V_0 = 260.7$ Å^3) was calculated from the corresponding lattice parameters, obtained by an extrapolation of their pressure dependences (Wakabayashi *et al* 1968) to $P = 0$ GPa. Table 4 lists the scaled TO and LO phonon-mode frequencies ω_s for orthorhombic PbTe. We denote $x = a$, $y = b$, $z = c$.

The compound CsCl does not belong to A^4B^6-type compounds and the scaled value $(\omega_{TO})_{BCC}$ for BCC PbTe was not calculated from equation (5) but from the relation

$$(\omega_{TO})_{BCC}/(\omega_{TO})_{FCC} = [(r_{Pb\text{-}Te})_{BCC}/(r_{Pb\text{-}Te})_{FCC}]^{-3/2} \tag{6}$$

where $(\omega_{TO})_{BCC}$ is the TO phonon frequency in the NaCl-type phase, and $(r_{Pb\text{-}Te})_{FCC}$ and

Table 4. Phonon frequencies in orthorhombic PbTe.

	$E \parallel a$				$E \parallel b$				$E \parallel c$			
		ω_{exp} (cm^{-1}) for the following samples				ω_{exp} (cm^{-1}) for the following samples				ω_{exp} (cm^{-1}) for the following samples		
Mode	ω_s (cm^{-1})	1010	0910	1411	ω_s (cm^{-1})	1010	0910	1411	ω_s (cm^{-1})	1010	0910	1411
TO_1	53	46	46	46	37	—	—	—	—	—	—	—
LO_1	57	—	—	—	38	—	—	—	—	—	—	—
TO_2	83	118	118	122	87	84	84	84	—	—	—	—
LO_2	100	—	—	—	95	—	—	—	—	—	—	—
TO_3	101	134	134	136	96	104	104	105	64	92	92	95
LO_3	121	—	—	—	128	—	—	—	—	—	—	—

Table 5. Phonon frequencies in FCC and BCC PbTe.

	ω (usually cited) (cm^{-1})	ω_s (cm^{-1})	ω_{exp} (our results) (cm^{-1})
NaCl type			
TO	32	—	32
LO	114	—	109
CsCl type			
TO	—	49	50

$(r_{Pb\text{-}Te})_{BCC}$ are the interatomic distances in the corresponding phases (Fujii *et al* 1984). The scaled value of ω_{TO} for BCC PbTe is given in table 5.

A tentative mode assignment for orthorhombic PbTe (table 4) was obtained by scaling the mode frequencies and taking into account also

(i) our results from the x-ray investigation and

(ii) the experimental values of the Raman-active modes in the HP phases (Ves *et al* 1989).

The difference between the values ω_s and the measured phonon frequencies ω_{exp} reaches 30 cm^{-1}. Taking into account that the GeS-type phase pressure coefficients $d\omega/dP$ for the Raman-active modes vary from -0.68 to 2.24 cm^{-1} GPa^{-1} (Ves *et al* 1989) and that an orthorhombic PbTe phase takes place at pressures from 5 to about 16 GPa, the agreement between ω_{exp} and ω_s is good enough. The latter explains the slightly higher values of some mode frequencies in the thinnest sample (sample 1411), too.

4. Conclusion

X-ray investigations of PbTe/KCl films grown by LAD showed that the strained layers in these films consisted of HP phases with GeS- and CsCl-type structures. We have demonstrated that the experimental FIR reflectance spectra can be successfully interpreted on the following assumptions:

(i) multiple reflectance from two absorbing sublayers on an absorbing substrate;

(ii) a resonant-like frequency dependence of the electron damping parameter, interpreted as a result of an electron scattering off potential wells, formed by dislocations.

From the quantitative interpretation of the FIR spectra we obtained

(i) the frequencies of the infrared-active TO modes in PbTe with GeS- and CsCl-type crystal structures (the modes were tentatively assigned by scaling of the corresponding SnSe and FCC PbTe frequencies) and

(ii) the energies of the bound states in the potential wells, formed by dislocations.

Acknowledgments

The work has been financially supported by the National Science Committee under Contract 118. The authors are indebted to Mrs V Gaidarova for growing the samples, and to Mr M Giulmesov for taking the FIR spectra.

References

Baleva M I 1986 *Thin Solid Films* **139** L71
Barth W, Elsaesser K and Guth W 1976 *Phys. Status Solidi* a **34** 153
Bruesch P 1986 *Phonons: Theory and Experiments II (Springer Ser. Solid-State Sci. 65)* (Berlin: Springer) p 26
Burkhard H, Bauer G and Lopez-Otero A 1976 *Solid State Commun.* **18** 773
—— 1977 *J. Opt. Soc. Am.* **67** 943
—— 1978 *Phys. Rev.* B **18** 2935
Chandrasekhar H R, Humphreys R G, Zwick U and Cardona M 1977 *Phys. Rev.* B **15** 2177
Chattopadhyay T, von Schering H G, Gresshaus W and Holzapfel W B 1986 *Physica* B + C **139–40** 356
Fujii Y, Kitamura K, Onodera A and Yamada Y 1984 *Solid State Commun.* **49** 135
Katayama S, Mills D and Sirko R 1983 *Phys. Rev.* B **28** 6079
Kondrashov V E 1976 *Optika Fotocatodov* (Moscow: Nauka)
Perkowitz S 1975 *Phys. Rev.* B **12** 3210
Ridley B K 1986 *Quantum Process in Semiconductors* (Moscow: Mir) p 173 (in Russian)
Ves S, Pusep Yu A, Syassen K and Cardona M 1989 *Solid State Commun.* **70** 257
Wakabayashi I, Kobayashi H, Nagasaki H and Minomura S 1968 *J. Phys. Soc. Japan* **25** 227